

4-2013

Graphene: An effective oxidation barrier coating for liquid and two-phase cooling systems

Arun S. Kousalya

Birck Nanotechnology Center, Purdue University, aselvar@purdue.edu

Anurag Kumar

Birck Nanotechnology Center, Purdue University, kumar50@purdue.edu

Rajib Paul

Birck Nanotechnology Center, Purdue University, paul24@purdue.edu

Dmitry Zemlyanov

Birck Nanotechnology Center, Purdue University, dimazemlyanov@purdue.edu

Timothy S. Fisher

Birck Nanotechnology Center, Purdue University, tsfisher@purdue.edu

Follow this and additional works at: <http://docs.lib.purdue.edu/nanopub>



Part of the [Nanoscience and Nanotechnology Commons](#)

Kousalya, Arun S.; Kumar, Anurag; Paul, Rajib; Zemlyanov, Dmitry; and Fisher, Timothy S., "Graphene: An effective oxidation barrier coating for liquid and two-phase cooling systems" (2013). *Birck and NCN Publications*. Paper 1375.
<http://dx.doi.org/10.1016/j.corsci.2012.12.014>

This document has been made available through Purdue e-Pubs, a service of the Purdue University Libraries. Please contact epubs@purdue.edu for additional information.



Letter

Graphene: An effective oxidation barrier coating for liquid and two-phase cooling systems

Arun S. Kousalya, Anurag Kumar, Rajib Paul, Dmitry Zemlyanov, Timothy S. Fisher*

School of Mechanical Engineering and Birk Nanotechnology Center, Purdue University, West Lafayette, IN 47907, USA

ARTICLE INFO

Article history:

Received 30 November 2012

Accepted 18 December 2012

Available online 28 December 2012

Keywords:

A. Graphene

C. Boiling

C. Oxidation

A. Copper

ABSTRACT

Graphene is studied as an oxidation barrier coating for liquid and liquid–vapor phase-change cooling systems. Forced convection heat transfer experiments on bare and graphene-coated copper surfaces reveal identical liquid-phase and two-phase thermal performance for the two surfaces. Surface analysis after thermal testing indicates significant oxide formation on the entire surface of the bare copper substrate; however, oxidation is observed only along the grain boundaries of the graphene-coated substrate. Results show that few-layer graphene can act as a protective layer even under vigorous flow boiling conditions, indicating a broad application space of few-layer graphene as an ultra-thin oxidation barrier coating.

© 2012 Elsevier Ltd. All rights reserved.

Graphene, an allotrope of carbon, has emerged as a prominent two-dimensional material with numerous potential applications [1]. It comprises of a single-atom thick planar sheet of sp^2 -bonded carbon atoms in a honeycomb lattice and possesses unique properties that are essential in niche applications such as high electrical and thermal conductivity and exceptional mechanical strength. Over the past few years, improvements in graphene synthesis have resulted in new application possibilities. Currently, chemical vapor deposition (CVD) is the most common technique for single and few-layer graphene synthesis on metal substrates [2–4]. Transfer of graphene film from the growth substrates to various substrates has also been enabled by a PMMA-based transfer technique [2].

Several groups have demonstrated the effectiveness of graphene as a protective coating. Chen et al. [5] reported a CVD graphene coating as a diffusion barrier and an oxidation resistant layer for Cu and Cu/Ni alloy surfaces exposed to atmospheric air up to 4 h at temperatures as high as 200 °C. Long-term exposure (2 days) to the atmosphere showed oxidation to some extent throughout the foil along with significant oxidation along grain boundaries. Graphene coatings also provided substantial protection to Cu and Cu/Ni alloys exposed to an oxidizing aqueous solution of H_2O_2 , although only short duration exposure was investigated (less than 15 and 45 min for Cu/Ni alloy and Cu, respectively). Prasai et al. [6] demonstrated significant reduction in corrosion rates of graphene-coated Cu and Ni in aerated Na_2SO_4 solution. Corrosion of metal was found to occur predominantly at cracks in the graphene film. Kirkland et al. [7] investigated electrochemical corrosion resistance

of graphene-coated Cu and Ni in aqueous media and demonstrated that few-layer graphene coatings significantly reduce the rate of corrosion in pure metals.

Rafiee et al. [8] recently reported another unique aspect of graphene as a protective coating. When metals such as gold and copper were coated with less than three graphene layers, they exhibited no change in their intrinsic surface wetting behavior. This so-called ‘wetting transparency’ was observed only when van der Waals forces dominated surface–water interactions such as in gold and copper as opposed to glass for which short-range chemical bonding predominates surface wetting. However, when more than six layers of graphene were present on these metals, the contact angle was found to reach the bulk graphite value of 94°. Condensation heat transfer experiments performed on graphene-coated copper revealed ~30–40% improvement in overall condensation heat transfer coefficient over a wide temperature range [8]. The graphene coating was unique in the sense that it can prevent copper oxidation while the intrinsic surface wetting remains unaltered. In another work, Rafiee et al. [9] reported a facile technique to control the surface wettability of thermally exfoliated graphene films by controlling the relative proportion of acetone and water in the solvent during ultrasonication. Contact angles ranging from 150° (superhydrophobic) to less than 10° (superhydrophilic) were demonstrated using acetone and water as a solvent, respectively.

However, a detailed investigation on long-term exposure of graphene-coatings to oxidizing/corrosive liquid media has not been reported. In most industrial applications, oxidation and corrosion protection coatings are exposed almost indefinitely to the working liquids. Hence, verification of the long-term oxidation

* Corresponding author. Tel.: +1 765 494 5627.

E-mail address: tsfisher@purdue.edu (T.S. Fisher).

resistance of graphene coatings is essential for practical use. The focus of the current work is to assess graphene as an oxidation barrier coating upon long-term exposure to the working environment in common liquid and liquid–vapor phase-change cooling systems. In two-phase cooling systems, the adhesion strength of graphene to the underlying substrate should be high enough to withstand recurring forces resulting from continuous bubble departure from the boiling surface.

In designing liquid-cooling systems such as liquid heat exchangers and two-phase evaporators such as forced convection boiling systems, fouling presents a major challenge. Fouling is a process by which unwanted material (typically with a low thermal conductivity) deposits on the heat transfer surface, increasing the thermal resistance [10]. Further, the resulting small change in the diameter of the tube/channel can result in substantial decrease in flow rate or increment in pressure drop across the heat transfer equipment [11]. The costs associated with heat exchanger fouling are estimated at about 0.25% of the GDP of many industrialized countries [12]. A number of factors contribute to fouling, such as corrosion, oxidation, particulates, precipitation and biological growth [10]. Aside from an induction period (an initial period of no significant fouling), thermal resistance to heat transfer continuously increases over time due to fouling. A number of techniques exist to mitigate fouling, such as fouling-resistant fluid additives, exposure to electric fields [11], adjustment of the hydrodynamic flow conditions using pulsation [13], and surface engineering of fouling-resistant coatings [13,14]. A moderation of fouling rates can reduce the surplus surface area often provided in heat exchangers to account for the decrease in heat transfer rates associated with fouling [10]. In the design of passive phase-change cooling systems, surface oxidation of sintered metal powder wicks over time often leads to reduced capillary pressures due to increase in contact angles, resulting in limited heat flux bearing capability [15,16].

The unique characteristics of a graphene film such as efficient heat spreading [17], wetting transparency [8], surface wetting tunability [9], chemical inertness, along with oxidation [5] and corrosion resistance [6,7] makes it an appealing fouling- and oxidation-resistant coating for pumped liquid cooling and passive phase-change cooling technologies. Two nominally identical oxygen-free copper substrates were prepared in this study to test the efficacy of the graphene as an oxidation barrier coating. The inset in Fig. 1 shows a schematic of the copper substrate. The dimensions of the copper substrate were such that they fit into

the flow-boiling cell depicted in Fig. 1. The area of the top surface was $17.5 \times 17.5 \text{ mm}^2$ while the entire copper substrate was 9 mm high. The top surfaces were mirror-finished in order to obtain identical surface roughness ($R_a < 100 \text{ nm}$) and cavity distribution, characteristics that are well known to influence single-phase and boiling heat transfer [18]. A scanning electron microscopy (SEM) image of the mirror-finished copper substrate obtained using a Hitachi S-4800 field emission microscope is presented in Fig. 2(a). A SEM image of a $25 \mu\text{m}$ thick copper foil, a commonly used substrate for CVD growth of graphene, is provided in the inset of Fig. 2(a) for surface roughness comparison. Graphene growth on the copper substrate was carried out in a SEKI AX5200S microwave plasma chemical vapor deposition (MPCVD) system. The graphene synthesis procedure is identical to that reported in a previous study [3] and is described in Supplemental information.

Raman spectroscopy of graphene on the copper substrate was performed using a Renishaw Raman microscope with 633 nm excitation wavelength, 2 mW laser power and $100\times$ magnification. Fig. 3(a) shows the Raman spectrum of graphene displaying a D peak near 1330 cm^{-1} , a G peak near 1580 cm^{-1} , a D' peak near 1620 cm^{-1} , and a 2D peak near 2660 cm^{-1} . Zone-boundary phonon scattering caused by defects contributes to D and D' peaks while the second order resonance of the D peak contributes to the 2D peak [19]. The G peak appears due to planar vibrations in the crystalline graphitic material. The ratio of the D and G intensities ($I(D)/I(G) = 1.74$) reveals the defective nature of graphene. The highly energetic radicals in the microwave plasma cause defects in graphene [3]. The D peak intensity is further accentuated by the long wavelength (633 nm) laser used in the study. D and 2D peaks in graphene have been shown to be dispersive [20]. With increasing laser wavelength, the peak positions of the D and 2D peak undergo a progressive red shift while the corresponding peak intensities are also enhanced. Graphene grown on Cu foil under similar conditions [3] has been shown to have 4–8 layers, and a film of similar thickness is expected to be obtained over a Cu block as well.

Contact angle experiments were conducted on bare and graphene-coated copper substrates using a Ramé-Hart digital goniometer model 290. A Hamilton micro-syringe was used for dispensing $3 \mu\text{l}$ sessile deionized water droplets. Eight contact angle measurements were conducted on different areas of each substrate. Prior to thermal testing, the contact angle of bare copper substrate was measured to be $93.7 \pm 1.7^\circ$, whereas the contact angle of graphene-coated copper substrate was $71.8 \pm 1.2^\circ$. The optical images corresponding to contact angle experiments are presented in Supplemental information (Fig. S1). Because more than three layers of graphene were expected to be present, the contact angle on the graphene-coated substrate was anticipated to reach the bulk graphite value of 94° [8]. However, the observed reduction in contact angle is likely due to the defective nature of the graphene and charge states at the micron-size grain boundaries of graphene [21].

The flow loop used to evaluate boiling characteristics of bar and graphene-coated substrates is portrayed in Fig. 4. Ultra-pure water, used as the working fluid, was supplied to the flow loop from a central water treatment system. A $15 \mu\text{m}$ filter prevents entry of unwanted particles, and a flowmeter (Mcmillan 106-5-D-T4) records the volumetric flow rate. Water, initially at room temperature, is heated by the inline heater (Omega AHPF-121) to an inlet temperature of $59.5 \pm 0.5^\circ\text{C}$ at the boiling test module. T-type thermocouples installed in the inlet and the outlet plenums are used to measure the inlet and outlet water temperatures. The central flow cell contains a rectangular fluid flow channel with inlet and outlet plenums. An orifice in the center of the flow cell allows for assembling the top surface of the test substrate. A cover plate houses a $38 \text{ mm} \times 38 \text{ mm} \times 3 \text{ mm}$ thick quartz window at its center, facilitating flow visualization during thermal testing. A silicone

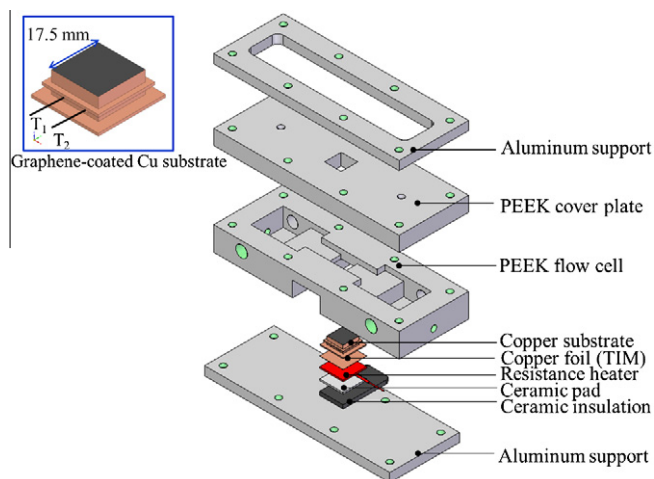


Fig. 1. Schematic of the flow boiling test module. Inset shows a schematic of the graphene-coated copper substrate.

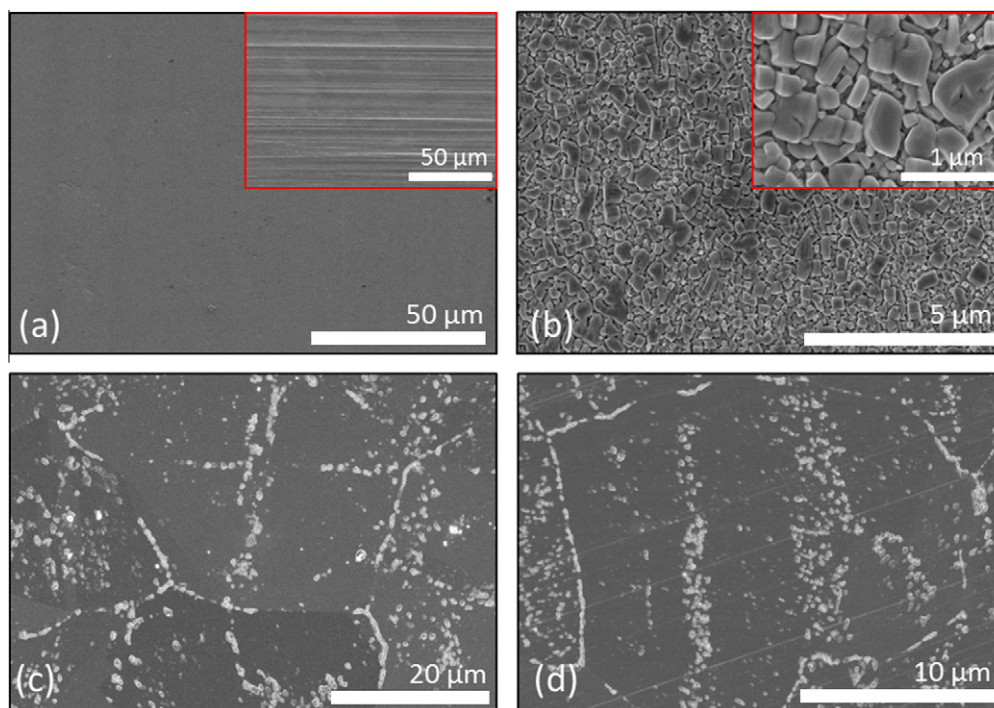


Fig. 2. SEM image showing (a) mirror-finish bare copper substrate before thermal testing (inset: SEM image of a 25 μm copper foil), (b) copper oxide formation on bare copper substrate after thermal testing (inset: high-magnification image of copper oxide crystals) and copper oxidation predominantly along the grain boundaries of graphene film on (c) mirror-finish and (d) roughened copper substrate.

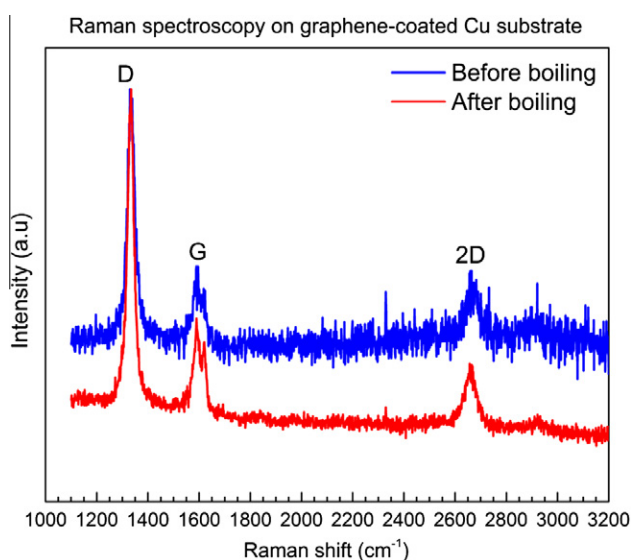


Fig. 3. Raman spectrum of graphene-coated copper substrate before and after thermal testing.

O-ring placed between the cover plate and the flow cell ensures a leak-tight seal. Test substrates were bonded to the flow cell utilizing a RTV silicone sealant. The dimensions of the copper substrate ensure that the sample is flush with bottom surface of the flow cell to prevent any water leak during testing.

A resistance heater (Watlow Ultramic 240 V, 967 W) connected to an external power supply (Sorensen DHP 300) supplies heat to the sample. Thermal contact resistance between the heater and the sample is reduced by inserting a 25 μm copper foil. The top and bottom aluminum plates provide for support and rigidity. A high-temperature ceramic tape and a ceramic block insulate the

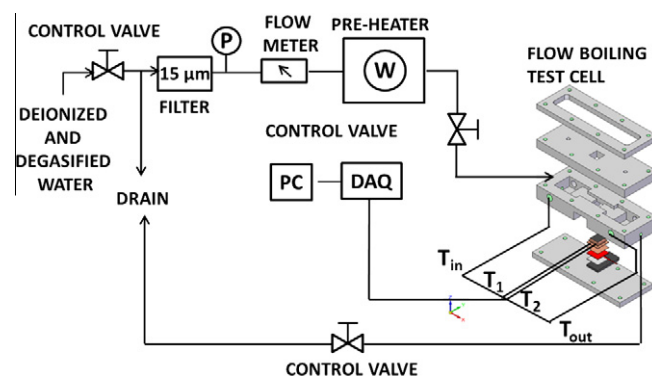


Fig. 4. Schematic of the flow boiling experimental test loop.

heater from the bottom aluminum plate. Bolt fasteners hold the entire test module together. Copper substrate temperatures are recorded by two T-type thermocouples placed symmetrically. The inlet fluid pressure is measured by an absolute pressure transducer from Omega (PX409-050A5V) and consistently reported levels close to atmospheric pressure during all experiments. The fluid and copper substrate temperatures and the inlet pressure are measured by a Keithley 2601 data acquisition (DAQ) system interfaced to a personal computer.

The inlet fluid temperature and volumetric flow rate were maintained at 59.5 ± 0.5 $^{\circ}\text{C}$ and 222 ml/min, respectively, during all flow boiling tests. A relatively low volumetric flow rate was employed to ensure laminar flow, yielding a Reynolds number $Re \approx 675$ and a mass velocity $G \approx 38$ $\text{kg/m}^2 \text{s}$ (based on the ratio of mass flow rate and the cross sectional area of the channel). The flow boiling system was flushed with degasified water for at least 60 min. Once steady state conditions were confirmed, the power to the resistive heater was incremented to a point of

vigorous boiling. The system was left for at least 30 min under this condition before reducing the heater power to zero. Thereafter, at each increment, the system was allowed to reach steady-state before thermal data were recorded. The steady-state temperature data reported are averages of 100 readings. A standard procedure was adopted for obtaining the boiling curves and estimating the heat flux reaching the boiling surface [22].

Six flow-boiling experiments were conducted (T1–T6): three experiments on bare copper (T1–T3) and three on graphene-coated copper (T4–T6). Both single-phase (liquid) heat transfer coefficients and two-phase flow-boiling curves were obtained from each of the six experiments. Once each substrate was assembled into the central flow cell, a continuous supply of water at an inlet temperature of $59.5 \pm 0.5^\circ\text{C}$ was allowed to flow in the rectangular channel until all the three flow-boiling test runs were completed. Each flow boiling test run lasted between 5 and 6 h, and a single run was conducted in a day. When boiling runs were not performed, the heater power was restored back to zero while the inlet water temperature was kept constant at $59.5 \pm 0.5^\circ\text{C}$. After the completion of three runs, the substrate was disassembled and stored in a nitrogen dry box kept in a cleanroom to prevent oxidation. Overall, each substrate was maintained at more than 100°C for at least 9 h. Fig. 5 compares the thermal characteristics obtained for all six test runs on the two mirror-finished copper substrates, one with and one without the graphene coating.

The six curves reveal that the heat transfer characteristics of the two substrates are similar and within the experimental uncertainties for most test points, both in the single-phase and two-phase flow regimes. These results demonstrate that the ultra-thin graphene coating did not alter the thermal performance of the surface in either regime. In general, hydrophobic surfaces initiate boiling at relatively low surface temperatures compared to hydrophilic surfaces due to the lower surface superheat required for vapor embryo growth [18]. An increase in surface roughness also results in earlier incipience of boiling [23]. Based on the results of contact angle experiments (Fig. S1) and thermal testing (Fig. 5), we hypothesize that the increase in surface roughness of graphene-coated substrate [9] compensated for its hydrophilic nature (as determined by contact angle experiments) leading to similar boiling incipience superheat and heat transfer coefficients as that of a bare copper substrate.

Similar flow-boiling tests (T7–T8) were performed on two substrates roughened with a 600 grit sandpaper, one with and the

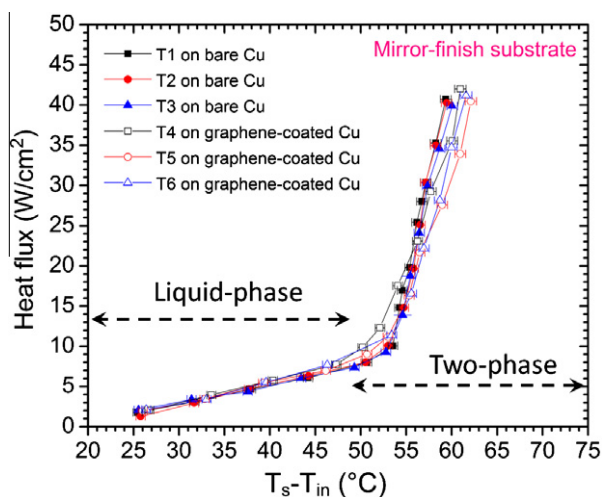


Fig. 5. Flow boiling curves for mirror-finished bare copper and graphene-coated copper surface with mass velocity $G \cong 38 \text{ kg/m}^2 \text{ s}$ and inlet fluid temperature $T_{\text{in}} = 59.5 \pm 0.5^\circ\text{C}$.

other without graphene coating, to assess the thermal performance of graphene coating on a rough surface. Identical single-phase and two-phase heat transfer coefficients were obtained for surface roughened copper substrates (Fig. S2 in Supplemental information), confirming that the thermal performance remains unaltered for rough surfaces as well. A comparison of Figs. 5 and S2 confirms that an increase in surface roughness leads to reduction in the surface temperature required for boiling incipience, as expected. The slope of the boiling curve also increases with surface roughness as anticipated.

Post-testing surface analysis on the mirror-finish copper substrates was performed using Raman spectroscopy, SEM, contact angle measurements and X-ray photoelectron spectroscopy (XPS). Digital images of bare (Fig. 6(a)) and graphene-coated (Fig. 6(b)) copper substrates after thermal testing shows retention of the 'shiny' copper surface by the graphene-coated substrate, whereas the bare substrate shows a blackish-red copper oxide hue. The Raman spectrum of graphene-coated sample after testing (Fig. 3(b)) reveals the presence of D, G and 2D peak signatures of graphene. The ratio of the D to G peak intensities before and after boiling (1.74 before testing, 2.25 after testing) reveals an increase in defect density of graphene after thermal testing. Both samples displayed an increase in contact angle after thermal testing. The contact angle on the bare copper substrate was found to be $112.7 \pm 3.9^\circ$ (Fig. S1(b)) while the graphene-coated substrate displayed a contact angle of $94.6 \pm 3.7^\circ$ (Fig. S1(d)). The hydrophobic nature of the bare copper substrate is due to the formation of the oxide thin film. The increase in contact angle of the graphene-coated substrate is likely due to oxide formation along the graphene grain boundaries.

SEM images taken after thermal testing revealed significant oxide formation on the entire surface of the bare copper substrate (Fig. 2(b)). A thin film of copper oxide covered the entire boiling surface. Cu_2O crystals of two sizes were observed (inset of Fig. 2(b)), one with extent of few hundreds of nanometers, the other of few tens of nanometers. Similar SEM analysis on the mirror-finish (Fig. 2(c)) and roughened (Fig. 2(d)) copper substrate coated with graphene revealed a small amount of oxidation, which is predominantly localized to the grain boundaries of graphene. Graphene grown on polycrystalline copper by CVD shows non-ideal characteristics such as point defects, wrinkles, cracks, and grain boundaries [5,6,24]. Surface analysis after experimental testing (Fig. 2(c) and (d)) suggests that the molecular diffusion of oxygen through the chemically active grain boundaries of CVD synthesized graphene is the dominant mechanism of oxidation. A similar observation was made by Chen et al. [5] with air as the oxygen source. Oxidation observed within a graphene grain is attributed to point defects [25] and cracks [6] within the graphene that have been suggested to act as nucleation sites for oxidation in prior work on CVD-grown graphene. The SEM images (Fig. 2(c) and (d)) reveal that the domain size of the graphene grains grown by MPCVD is of the order of few tens of microns.

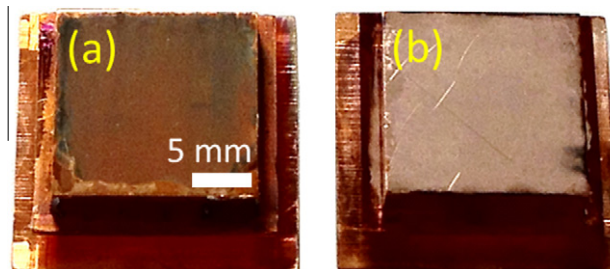


Fig. 6. Digital photograph of (a) bare and (b) graphene-coated mirror-finished copper substrate after thermal testing.

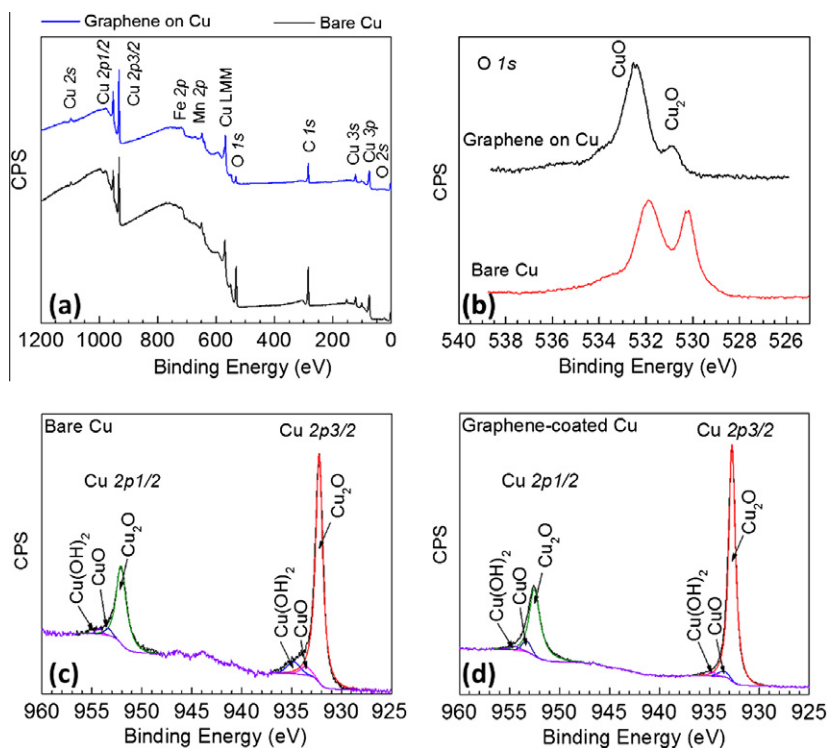


Fig. 7. (a) Post-boiling XPS survey spectra of mirror-finished copper substrate with and without graphene-coating. (b) Comparison of O 1s signatures of bare and graphene-coated copper substrate. (c) High resolution Cu 2p XPS spectra of bare and (d) graphene-coated copper substrate.

X-ray photoelectron spectroscopy (XPS) was utilized to investigate the chemical compositions of the Cu substrate with and without the graphene coating after thermal testing. A Kratos Ultra DLD spectrometer with monochromatic Al K α radiation ($h\nu = 1486.58$ eV) was used in this study. Survey and high-resolution spectra were recorded for a $700 \times 400 \mu\text{m}^2$ spot size irradiation at normal incidence with fixed analyzer pass energies of 160 and 20 eV, respectively. XPS data were analyzed with commercially available CasaXPS software (www.casaxps.com), and individual peaks were fitted with a Gaussian/Lorentzian (GL) function. The resulting spectra were corrected on the binding energy scale, using the C 1s peak position at 284.5 eV as a reference for graphitic carbon [26]. Fig. 7(a) compares the XPS survey spectra of copper substrate with and without graphene coating. The O 1s peak was more intense on the bare copper substrate compared to that with the graphene coating. The oxygen content on bare copper substrate was 30 at.% while that value reduced to 11 at.% for the copper substrate with graphene coating. This result clearly indicates that the oxidation process on the bare copper substrate surface proceeds at a faster rate. High-resolution O 1s and Cu 2p XPS spectra recorded for the copper substrates with and without graphene are shown in Fig. 7(b)–(d). Both copper substrates possess oxides in the form of Cu₂O and CuO; however the graphene-coated Cu substrate registered a low-intensity Cu₂O peak. The Cu 2p spectra contain two peaks, namely Cu 2p_{3/2} and Cu 2p_{1/2} (Fig. 7(c) and (d)) on both substrates. Further fitting of sub-shoulders under the each of these peaks reveals the presence of Cu₂O, and small proportions of CuO and Cu(OH)₂. The CuO proportion decreased from 3.7 at.% for the bare Cu to 1.4 at.% for the graphene-coated sample while the Cu₂O proportion remained almost unchanged. The Cu(OH)₂ proportion also reduced from 2.2 at.% in bare Cu to 0.6 at.% for graphene-coated Cu.

Although thermal performance degradation was not observed in the first three experimental runs due to an increase in surface roughness as a result of CuO formation (typical during the induc-

tion fouling period), the increase in thermal resistance due to scale formation is a common issue over long durations. The reported thermal conductivity of Cu₂O is 4.5 W/mK [27], approximately two orders of magnitude lower than that of copper and can result in significant increases in fouling resistance after the induction period.

The results indicate that even under long-term vigorous boiling conditions (up to 9 h), the graphene coating retains its chemical inertness and serves as an oxidation barrier coating, except along its grain boundaries. The graphene film strongly adheres to the underlying copper substrate and does not rupture when subjected to recurring forces of the bubble ebullition cycle. In order to decrease oxide formation further, it is imperative to synthesize defect-free large-domain graphene films. Selection of the proper size and crystallographic orientation of copper grains has recently been shown to affect the quality of graphene films [28]. Thermal annealing of the copper substrate at high temperatures (~ 1035 °C) can also promote large domain sizes of graphene films [28].

Conclusion

In summary, we have demonstrated that graphene coating is stable under vigorous flow boiling conditions and can be used as an effective oxidation barrier coating for liquid and liquid–vapor cooling systems, even under long-term exposure to the working fluid.

Acknowledgements

Funding from the US Air Force Office of Scientific Research, Thermal Sciences (Program Manager: Dr. Joan Fuller) is gratefully acknowledged. We acknowledge Prof. Suresh V. Garimella and Prof. Jong H. Choi at Purdue University for allowing access to the

contact angle experimental setup and Raman spectroscopy equipment, respectively.

Appendix A. Supplementary data

Supplementary data associated with this article can be found, in the online version, at <http://dx.doi.org/10.1016/j.corsci.2012.12.014>.

References

- [1] A.K. Geim, K.S. Novoselov, The rise of graphene, *Nat. Mater.* 6 (2007) 183–191.
- [2] X. Li, W. Cai, J. An, S. Kim, J. Nah, D. Yang, R. Piner, A. Velamakanni, I. Jung, E. Tutuc, S.K. Banerjee, L. Colombo, R.S. Ruoff, Large-area synthesis of high-quality and uniform graphene films on copper foils, *Science* 324 (2009) 1312–1314.
- [3] A. Kumar, A.A. Voevodin, D. Zemlyanov, D.N. Zakharov, T.S. Fisher, Rapid synthesis of few-layer graphene over Cu foil, *Carbon* 50 (2012) 1546–1553.
- [4] A. Malesevic, R. Vitchev, K. Schouteden, A. Volodin, L. Zhang, G. Van Tendeloo, A. Vanhulsel, C. Van Haesendonck, Synthesis of few-layer graphene via microwave plasma-enhanced chemical vapour deposition, *Nanotechnology* 19 (2008) 305604.
- [5] S. Chen, L. Brown, M. Levendorf, W. Cai, S.-Y. Ju, J. Edgeworth, X. Li, C.W. Magnuson, A. Velamakanni, R.D. Piner, J. Kang, J. Park, R.S. Ruoff, Oxidation resistance of graphene-coated Cu and Cu/Ni alloy, *ACS Nano* 5 (2011) 1321–1327.
- [6] D. Prasai, J.C. Tuberquia, R.R. Harl, G.K. Jennings, B.R. Rogers, K.I. Bolotin, Graphene: corrosion-inhibiting coating, *ACS Nano* 6 (2012) 1102–1108.
- [7] N.T. Kirkland, T. Schiller, N. Medhekar, N. Birbilis, Exploring graphene as a corrosion protection barrier, *Corros. Sci.* 56 (2012) 1–4.
- [8] J. Rafiee, X. Mi, H. Gullapalli, A.V. Thomas, F. Yavari, Y. Shi, P.M. Ajayan, N.A. Koratkar, Wetting transparency of graphene, *Nat. Mater.* 11 (2012) 217–222.
- [9] J. Rafiee, M.A. Rafiee, Z.-Z. Yu, N. Koratkar, Superhydrophobic to superhydrophilic wetting control in graphene films, *Adv. Mater.* 22 (2010) 2151–2154.
- [10] J.W. Saito, W.J. Marner, R.B. Ritter, The history and status of research in fouling of heat exchangers in cooling water service, *Can. J. Chem. Eng.* 55 (1977) 374–380.
- [11] Y.I. Cho, B.-G. Choi, Validation of an electronic anti-fouling technology in a single-tube heat exchanger, *Int. J. Heat Mass Transfer* 42 (1999) 1491–1499.
- [12] H. Müller-Steinhagen, M.R. Malayeri, A.P. Watkinson, Fouling of heat exchangers – new approaches to solve an old problem, *Heat Transfer Eng.* 26 (2005) 1–4.
- [13] M. Förster, W. Augustin, M. Bohnet, Influence of the adhesion force crystal/heat exchanger surface on fouling mitigation, *Chem. Eng. Process.: Process Intensification* 38 (1999) 449–461.
- [14] M.Y. Liu, H. Wang, Y. Wang, Enhancing flow boiling and antifouling with nanometer titanium dioxide coating surfaces, *AIChE J.* 53 (2007) 1075–1085.
- [15] A.P. Boyes, A.B. Ponter, Wettability of copper and polytetrafluoroethylene surfaces with water – the influence of environmental conditions, *Chem. Ing. Techn.* 45 (1973) 1250–1256.
- [16] G.V. Kuskov, Y.F. Maidanik, Macroscopic boundary angles of wetting of sintered capillary structures of heat pipes, *J. Eng. Phys. Thermophys.* 50 (1986) 53–58.
- [17] A.A. Balandin, Thermal properties of graphene and nanostructured carbon materials, *Nat. Mater.* 10 (2011) 569–581.
- [18] V.P. Carey, *Liquid Vapor Phase Change Phenomena*, second ed., Taylor & Francis, 2008.
- [19] D. Graf, F. Molitor, K. Ensslin, C. Stampfer, A. Jungen, C. Hierold, L. Wirtz, Spatially resolved Raman spectroscopy of single- and few-layer graphene, *Nano Lett.* 7 (2007) 238–242.
- [20] R.P. Vidano, D.B. Fischbach, L.J. Willis, T.M. Loehr, Observation of Raman band shifting with excitation wavelength for carbons and graphites, *Solid State Commun.* 39 (1981) 341–344.
- [21] A. Mesaros, S. Papanikolaou, C.F.J. Flipse, D. Sadri, J. Zaanen, Electronic states of graphene grain boundaries, *Phys. Rev. B* 82 (2010) 205119.
- [22] A.S. Kousalya, C.N. Hunter, S.A. Putnam, T. Miller, T.S. Fisher, Photonically enhanced flow boiling in a channel coated with carbon nanotubes, *Appl. Phys. Lett.* 100 (2012) 071601–071604.
- [23] B.J. Jones, J.P. McHale, S.V. Garimella, The influence of surface roughness on nucleate pool boiling heat transfer, *J. Heat Transfer – Trans. ASME* 13 (1) (2009) 14.
- [24] C. Mattevi, H. Kim, M. Chhowalla, A review of chemical vapour deposition of graphene on copper, *J. Mater. Chem.* 21 (2010) 3324–3334.
- [25] D.L. Duong, G.H. Han, S.M. Lee, F. Gunes, E.S. Kim, S.T. Kim, H. Kim, Q.H. Ta, K.P. So, S.J. Yoon, S.J. Chae, Y.W. Jo, M.H. Park, S.H. Chae, S.C. Lim, J.Y. Choi, Y.H. Lee, Probing graphene grain boundaries with optical microscopy, *Nature* 490 (2012) 235–U242.
- [26] R. Paul, A.A. Voevodin, D. Zemlyanov, A.K. Roy, T.S. Fisher, Microwave-assisted surface synthesis of a boron–carbon–nitrogen foam and its desorption enthalpy, *Adv. Funct. Mater.* 22 (2012) 3682–3690.
- [27] H. Timm, J. Janek, On the Soret effect in binary nonstoichiometric oxides – kinetic demixing of cuprite in a temperature gradient, *Solid State Ionics* 176 (2005) 1131–1143.
- [28] Z.R. Robinson, P. Tyagi, T.M. Murray, C.A. Ventrice, S. Chen, A. Munson, C.W. Magnuson, R.S. Ruoff, Substrate grain size and orientation of Cu and Cu–Ni foils used for the growth of graphene films, *J. Vac. Sci. Technol. A: Vac. Surf. Films* 30 (2011) 011401–011407.